Draft version December 15, 2019
Typeset using LaTeX **preprint** style in AASTeX61

TRANSIT OBSERVATION OF THE HOT JUPITER HAT-P-23B

Matthew Murphy,[1] Brianna Isola,[1] and Tyler Nill[1]

[1]*Department of Physics & Astronomy, Stony Brook University, Stony Brook, NY*

ABSTRACT

Transit events offer a unique opportunity to directly measure the radius of a planet relative to that of its host star. Follow up observations of detected transits are crucial to confirm or refine radius measurements of the transiting planet, which have implications in constraining theories of planetary formation. We present optical photometric measurements of one transit of the exoplanet HAT-P-23b. Observations were made using the 14-in telescope of Mt. Stony Brook Observatory with an optical R filter. We determine a transit duration of (2.20 ± 0.09) hours, a transit depth of $(1.366 \pm 0.018)\%$, and a planet-star radius ratio of 0.1169 ± 0.0008. Each of these measurements is consistent to within 0.36σ of previously observed transits of this planet.

1. INTRODUCTION

As of this report, over 4,000 exoplanets have been confirmed in over 3,000 star systems beyond our own[1]. The majority of these exoplanets are transiting: when viewed from Earth, the planet's orbit is edge-on and passes directly across the disk of its host star. As the exoplanet transits its host star, it will block a portion of the star's light. The amount of light that is blocked is proportional to the relative size of planet and star. This is known as the transit depth, which we denote as ϵ, and is given by

$$\epsilon = \left(\frac{R_p}{R_\star}\right)^2, \tag{1}$$

where R_p is the planet radius and $R_\star$ is the star radius. For a star of given radius, the depth of transit is quadratically proportional to the transiting planet's radius. Larger transit depths are easier to detect, so this transit method is more sensitive to large, massive planets. It is no coincidence that, early on, the majority of exoplanets detected via this transit method were gas giants.

The transit method is currently the most effective way to measure the radius of an exoplanet. Given the radius of the host star, which can be determined through optical interferometry or other methods, one only needs to measure the depth of transit to find the radius of the planet. Precise radius measurements are important because they can be combined with a measurement of the planet mass to calculate the planet's density. The internal composition of a planet is directly correlated to its density and understanding the compositions of exoplanets is crucial to constraining planetary formation processes. Therefore, it is prudent to follow up on and confirm detections of transiting exoplanets and obtain independent radius measurements.

In this work, we focus on the HAT-P-23 system. Discovered nearly a decade ago by Bakos et al. (2011), HAT-P-23b is a Hot Jupiter orbiting a G0 dwarf star. The system lies at an RA of $20^h24^m29.723^s$ and declination of $+16°45'43.81''$ with magnitude $V = 11.94$. The discovery report gives a radius of $R_p = 1.368\ R_J$ for the planet and $R_\star = 1.20\ R_\odot$ for the host star GSC 1632-01396. Several follow up measurements of this system have reported a smaller planet size. In particular, Ciceri et al. (2015) report a planet radius of $1.224\ R_J$ and Sada & Ramón-Fox (2016) report a planet size 4.5% smaller than the measurement at discovery.

HAT-P-23b is an interesting target because there is current debate on if the planet is an inflated Hot Jupiter, meaning it has a remarkably low density for a planet of its mass. Verification of this requires a combination of mass and radius measurements. Further, this planet is said to have one of the shortest in-fall times. It is expected to fall into its host star in roughly 7.5 Myr.

The layout of this report is as follows. In Sections 2 and 3 we describe our observational techniques and report photometric measurements of this system's light curve during a transit. The analysis of this light curve is detailed in Section 4 and our results are discussed and interpreted with respect to previous literature in Section 5.

2. DATA ACQUISITION

2.1. *Transit Prediction*

[1] *Facility:* Exoplanet Archive. https://exoplanetarchive.ipac.caltech.edu/index.html

Bakos et al. (2011) recorded a transit mid-point at T_C = JD 2454852.264 and report the planet to have a near-circular orbit with a period of $P = 1.21\ d$. Starting at T_C and iterating over the orbital period, we estimated that another transit would occur at a mid-point time of 02:56 UT on September 19, 2019. This corresponds to 22:56 EDT on September 18^{th}, local time in Stony Brook, NY.

We can also quickly estimate how long the transit will take. The transit duration is the time over which at least some part of the planet is in front of the host star, as viewed from Earth. In terms of the orbital period (P), the impact parameter (b), the orbital semi-major axis (a), and the stellar and planetary radii ($R_\star$ and R_p, respectively), the transit duration is

$$T_{dur} = \frac{P}{\pi} \arcsin\left(\frac{\sqrt{(R_\star + R_p)^2 - (bR_\star)^2}}{a}\right), \tag{2}$$

as derived by Wilson (2016). The impact parameter quantifies how much the planet's transit path is offset from the diameter of the star along that trajectory. A parameter of $b = 0$ means the planet transits directly across the center of its star. We calculate an upper limit on the duration by setting $b = 0$. For this estimate, we assume $P = 1.212884\ d$ and $R_p = 1.368\ R_J$ from Bakos et al. (2011), $a = 0.02302\ AU$ from Ciceri et al. (2015), and $R_\star = 1.29\ R_\odot$ from Tsantaki et al. (2014). These values give an upper limit duration estimate of $T_{dur} = 2.69\ h$. Centering this duration on our expected transit mid-point time, we get the expected transit ingress and egress at roughly 01:35 and 04:17 UT, respectively.

2.2. *Observing Equipment*

Observations were made using a 14-inch Meade LX200-ACF telescope operated by the Stony Brook University Department of Physics & Astronomy. This is a ground based telescope in Stony Brook, NY. The telescope was mounted with a SBIG STL-1001E CCD camera, which was set to use its imager camera. This CCD has a field of view of $24'$. The CCD was set to a temperature of $T_{CCD} = -10.0°C$ which varied by no more than $\pm 0.3°C$ throughout our observations. At this camera temperature we expect the dark current to be less than 1.635 $e^-/p/s$, based on previous work with the STL-1001E (Murphy et al. 2019).

The target star is type G0 so it peaks in the optical. This is ideal for our observing equipment which can only observe in the optical. The STL-1001E is equipped with five optical band filters. Since the STL-1001E is more sensitive at the red end of the optical spectrum and red light is least scattered in the atmosphere, we use the red band filter.

Based on the R_p and $R_\star$ measurements by Bakos et al. (2011), we expect a transit depth of $\epsilon \approx 0.0136$. The HAT-P-23 system is of apparent visual magnitude $V = 11.94$ so this translates to a transit signature of ≈ 0.16 mag. This is more than double the minimum variation able to be measured with our telescope and CCD, so we will certainly be able to detect the dip in the system's light curve due to the transit.

2.3. *Imaging Process*

All data was acquired in one observing run on the night of September 19, 2019. Details of the exposures taken are listed in Table 1. Observations of HAT-P-23 started about an hour before the expected ingress and were terminated about an hour after the expected egress, so that we would have a conclusive baseline for the out of transit flux. At 02:30 UT, imaging of the target was paused to

perform a GEM flip as the target crossed the meridian. This GEM flip took approximately fourteen minutes to conduct. Observations resumed at 02:44 UT and continued until the end of the observing period. The CCD was set to 1x1 binning for all images. Flat-fields were taken with AutoDark reduction and consisted of dome flats of the interior wall of the telescope dome after closing its shutters. Dark frames and images of the target were taken with no AutoDark reduction, so we manually correct for the dark current. The night sky was very clear this night but the Moon was roughly 80% illuminated, though it was $\approx 100^{\circ}$ from our target and did not affect measurements.

The stated exposure times were chosen to avoid saturating the CCD, which occurs at $\approx 65,000$ counts per pixel. The 60s exposure of our target gave $8,000 - 10,000$ counts per pixel on the target star and a maximum $\approx 35,000$ counts per pixel on the brightest stars in the FOV. The 2s exposure of our flat-fields gave an average $18,000 - 20,000$ counts per pixel across each image.

Table 1. Record of observations presented in this work. All exposures were taken at Mt. Stony Brook observatory on September 19, 2019, with respect to UT. N_{exp} represents the total number of exposures taken of that type.

Image / Target	Start Time (UT)	End Time (UT)	N_{exp}	Exposure [s]	Filter	AutoDark
HAT-P-23	00:39	04:54	226	60	R	N
Flat-field	05:08	05:09	10	2	R	Y
Dark frame	05:10	05:20	10	60	R	N

3. DATA REDUCTION

3.1. *Image Calibration and Extraction*

A master dark frame was constructed by median combining our series of ten dark frames. The average count value across this combined dark frame is $\approx 1,050$ per pixel. We subtract this master dark frame from each of our science images. Similarly, a dark-corrected master flat field was constructed by median combining our series of ten flat fields and normalized by the mode count value. The normalized pixel values on this master flat are ≈ 1.0 times the mode at the center of the image but decrease to ≈ 0.95 times the mode toward the edges, indicative of the CCD's decreasing sensitivity toward the edges. The dark corrected images are calibrated for this by dividing each pixel's count value by that pixel's corresponding value on the normalized flat field.

We solved the WCS of each science image using the Astrometry.net[2] service. Most of the target's light was encompassed within an image aperture of 8.137 pixels. This aperture size is larger than that which optimizes the SNR, but is more robust against seeing variations. The flux of each source on each image within this aperture was measured using SExtractor[3]. The flux and error on the flux for HAT-P-23 and ten reference stars were extracted. These reference stars were chosen based on having similar brightness and presence in every image.

3.2. *Lightcurve Calibration*

[2] http://astrometry.net/
[3] https://www.astromatic.net/software/sextractor

Table 2. The ten reference stars used in calibrating our light curve. Listed coordinates are of epoch J2000.

Object Name	RA [J2000]	Dec [J2000]
2MASS 20242555+1644376	20:24:25.55	+16:44:37.62
2MASS 20243646+1647060	20:24:36.47	+16:47:06.01
TYC 1632-1319-1	20:24:41.59	+16:46:28.17
2MASS 20242827+1642025	20:24:28.27	+16:42:02.58
TYC 1632-1019-1	20:24:36.17	+16:48:18.49
2MASS 20241441+1645374	20:24:14.42	+16:45:37.46
TYC 1632-1448-1	20:24:39.97	+16:42:26.05
2MASS 20244973+1643402	20:24:49.73	+16:43:40.29
2MASS 20242290+1647591	20:24:22.90	+16:47:59.15
2MASS 20241054+1641349	20:24:10.54	+16:41:33.55

We scale each reference star's flux f_j and error on the flux σ_{f_j} by that star's average flux $\langle f_j \rangle$ over the observing period. This scales each star's signal to scatter around 1.0 so that we may average them. Since our telescope is ground-based, the flux measurements are very sensitive to seeing, changes in airmass, and other atmospheric interference. We aim to correct for these by calibrating the target signal with respect to the scaled reference signals. In Figure 1, one can visualize the scatter of each star's $f_j/\langle f_j \rangle$ light curve. On this plot, curves are offset vertically to view them on the same axis.

No individual star exhibited variation that appeared significantly different than that of any other star. We reason that none of the stars had significant intrinsic brightness variation over the observation period and that all observed variation is a result of atmospheric effects. Some of the early exposures were significantly affected with fluxes being reduced by more than 2% from the typical value. A total of twelve exposures exhibited this and were subsequently removed from the analysis data.

The CCD used has a $24'$ field of view. Each star was situated near the center of this FOV, so they were all confined within a small area on the sky. Therefore, any atmospheric variation will have affected each star on the image equally. For each i^{th} image, we compute the weighted mean μ_i^{ref} and the corresponding error σ_i^{ref} of the flux measurements of the j reference stars.

$$\mu_i^{ref} = \frac{\sum_j f_j^{ref} / \left(\sigma_j^{ref}\right)^2}{\sum_j 1 / \left(\sigma_j^{ref}\right)^2} \tag{3}$$

$$\sigma_i^{ref} = \sqrt{\frac{1}{\sum_j 1 / \left(\sigma_j^{ref}\right)^2}} \tag{4}$$

The weighted mean takes into account the statistical weight of each star when averaging over the flux on each image. This reduces statistical noise and any systematic uncertainty due to previously undetected variability in brightness. Since atmospheric effects will have disrupted the signal from each star equally, scaling the flux of our target star relative to this weighted mean of the reference

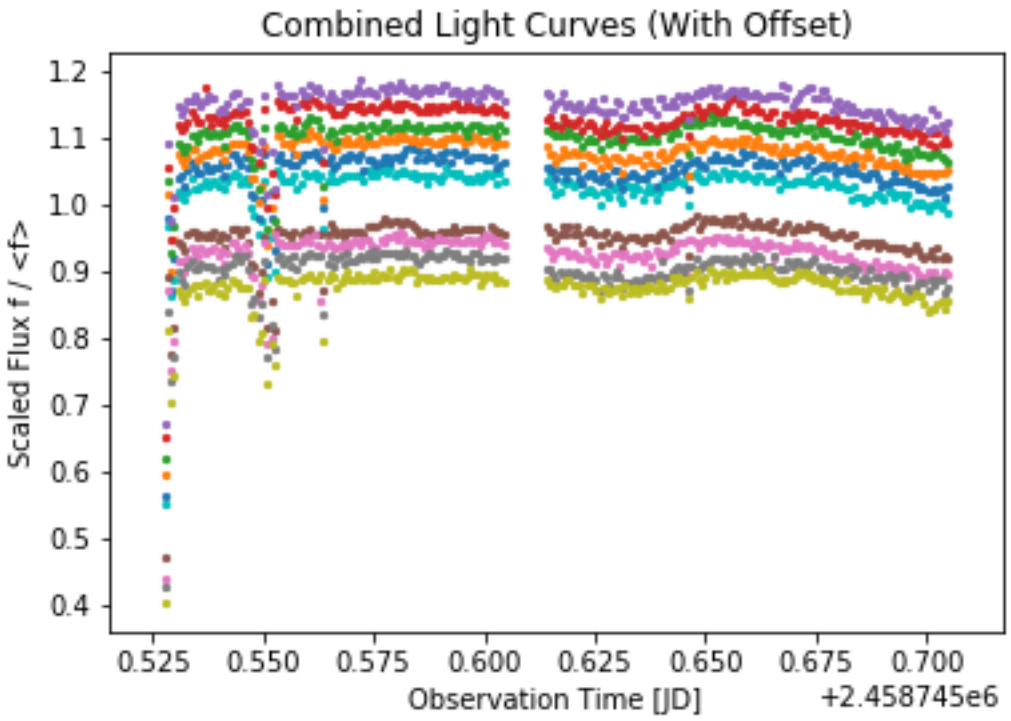

Figure 1. Scaled light curves $f/\langle f \rangle$ of the ten reference stars over the whole observing period. The curves are offset by a small constant so that they may be visualized on the same axis. The large gap near the middle of the observing period, in which there is no flux data for any star, is when the GEM flip was being performed.

stars effectively eliminates these adverse effects on the measurement. We calculate this scaling for each i^{th} image as $r_i = f_i^{sci}/\mu_i^{ref}$, where f_i^{sci} is the flux of HAT-P-23. The resulting r_i over the whole observing period is the target light curve, as shown in Figure 2.

4. ANALYSIS

The timing of our observations on September 19, 2019 were based on expected transit ingress at 01:35 UT and an expected egress at 04:17 UT, as we calculated in Section 2.1. These expected times do not match when the light curve of HAT-P-23 suggests the actual ingress and egress were, as shown in Figure 3. The curve suggests that the ingress occured at roughly 01:50 UT, given by the rightmost solid line in the figure, fifteen minutes after the expected time. Due to small variations in the raw light curve, we can not discern the exact start of transit within $\pm$ 3 minutes of this time, so this estimate carries judgement error. Adjusting the expected egress accordingly gives an new egress time of 04:02 UT, shown by the leftmost dashed line in the figure. The time between the adjusted ingress and egress times, accounting for the 3 minute uncertainty in determining these times, gives a transit duration of $T_{dur} = (2.20 \pm 0.09)$ h. Since this is less than the estimated duration time, we can assert that HAT-P-23b has a non-zero impact parameter.

We can clearly see a significant dip in the system's light curve indicative of the planet's transit. To determine the magnitude of this dip, the light curve must be normalized by the system's baseline flux. The baseline flux is the observed r when not in transit. There is a significant amount of

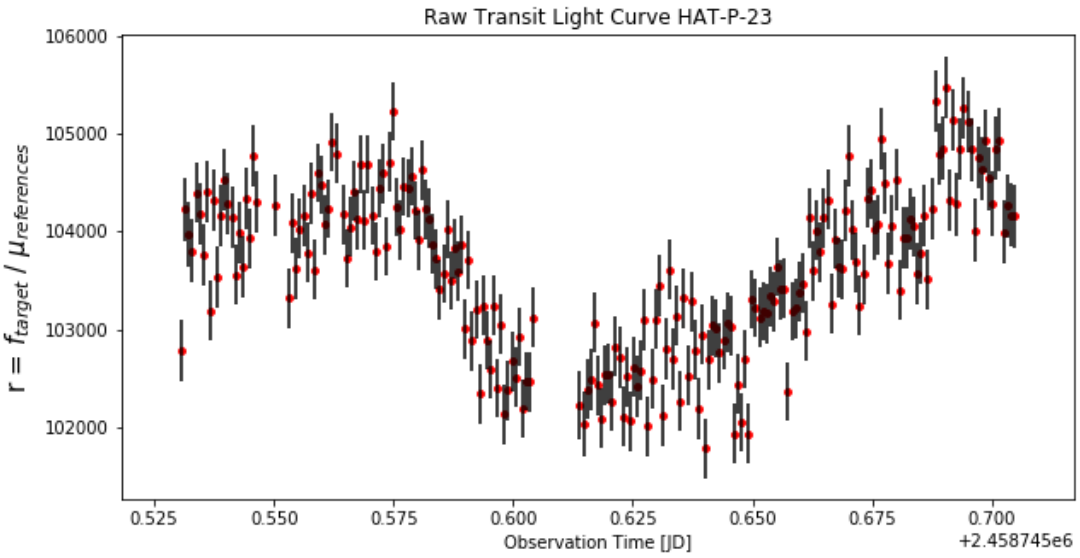

Figure 2. The unnormalized light curve of HAT-P-23 over the transit event as observed from the 14-in telescope at Stony Brook University. On the y-axis, the target flux has been scaled by the weighted mean of fluxes of ten reference stars. The gap in data near the transit midpoint was during a GEM flip of the telescope. We see a significant dip in the scaled flux during the middle of the observing period, this is the signature of the transiting exoplanet.

variation on the exit side of the transit light curve, so we will isolate only the exposures before the ingress. The mean $r_{baseline} \equiv \langle r \rangle$ of these exposures is the baseline flux, which we determine to be $r_{baseline} = 104140.9$. We then normalize r_i and its error by this baseline flux, resulting in the final transit light curve of Figure 4.

When the amount of the star's light blocked by the planet is at its maximum, the planet is said to be in full transit. That is, the stellar disk is obscured by the full body of the planet such that $r = 1 - \epsilon$, where ϵ is the transit depth. From our light curve, we estimate this to begin at 02:06 UT, 50 minutes prior to the transit mid-point. As with the ingress time, we can only judge this time to within $\pm$ 5 minutes. Similarly, it is difficult to discern when the planet exited the full transit state as there is considerable variation in r during the range of time when we would expect this to occur. Therefore, we estimate that the full transit ended 50 minutes after the mid-point at 03:46 UT.

To determine the transit depth, we must calculate the average values of r outside the transit (r_{base}) and during the full transit ($r_{transit} = r_{base} - \epsilon$). The star's baseline is roughly consistent before and after the transit. There is more variation, however, in the light curve after the transit. The flux measured before the transit is a better measure of the baseline, so we will use only these values for the calculation. To account for the error in determining the ingress time, we calculate r_{base} for several values of the time within the $\pm$ 3 minute interval and determine the average and deviation between them. In doing this, we determine the baseline to be $r_{base} = 1.0001 \pm 0.0002$. This is consistent with the expectation that r should scatter around 1.0 outside the flux, which motivated this normalization. The error in determining the exact start of full transit is accounted for in the same way, giving $r_{transit} = 0.9868 \pm 0.0001$. The difference of these gives a transit depth of $\epsilon = (1.333 \pm 0.022)\%$. From (1), this depth gives a planet-star radius ratio of $(R_p/R_\star) = 0.1154 \pm 0.0009$.

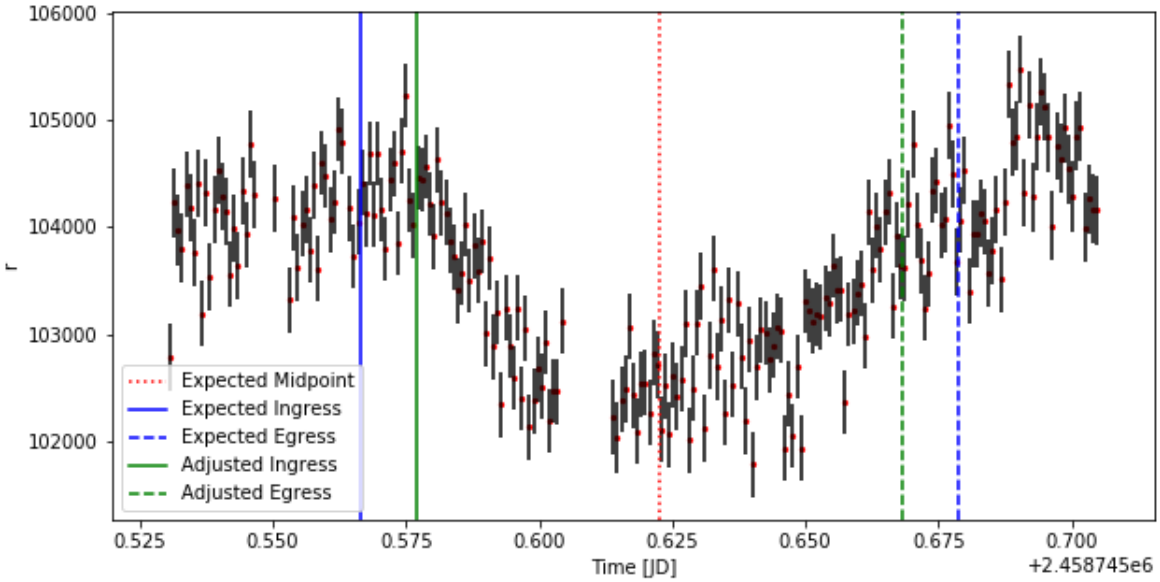

Figure 3. Transit light curve of HAT-P-23b viewed from the 14-in telescope at Stony Brook University, as in Figure 2, but with ingress, mid-point, and egress times overlayed. The two solid lines represent ingress: the leftmost solid line is the expected ingress time calculated from (2), and the rightmost solid line is the actual ingress time determined from the light curve. The central dotted line is the expected transit mid-point. The dashed lines represent egress: the leftmost dashed line is now the actual egress determined from the difference between actual ingress and midpoint, and the rightmost dashed line is the expected egress calculated from (2). We determine the transit duration to be $T_{dur} = (2.20 \pm 0.09)h$, less than our upper limit estimate.

5. DISCUSSION

HAT-P-23 is a system consisting of a G0 dwarf star and a transiting Hot Jupiter. Based on the reported transit time and period from the initial discovery report (Bakos et al. 2011), we predicted another transit would occur at 02:56 UT on September 19, 2019. We observed one transit of this planet using the 14-inch Meade LX200-ACF telescope at Stony Brook University with a STL-1001E CCD and an R-band optical filter. From the resulting light curve of this transit event, we determined the transit duration, transit depth, and ratio of the planet's radius to that of the host star. Our measurements are presented in Table 3 alongside literature values.

Table 3. Presentation of our measurements from the transit of HAT-P-23b on Sep. 19, 2019, listed alongside literature values measures from previous transits.

	This work	Bakos et al. (2011)	Ciceri et al. (2015)	Sada & Ramón-Fox (2016)
Duration	(2.20 ± 0.09) h	(2.17 ± 0.02) h		
Transit Depth	$(1.333 \pm 0.022)\%$	$(1.364 \pm 0.238)\%$	$(1.325 \pm 0.001)\%$	
$R_p/R_\star$	0.1154 ± 0.0009	0.1168 ± 0.0102	0.1151 ± 0.0047	0.1115 ± 0.0097

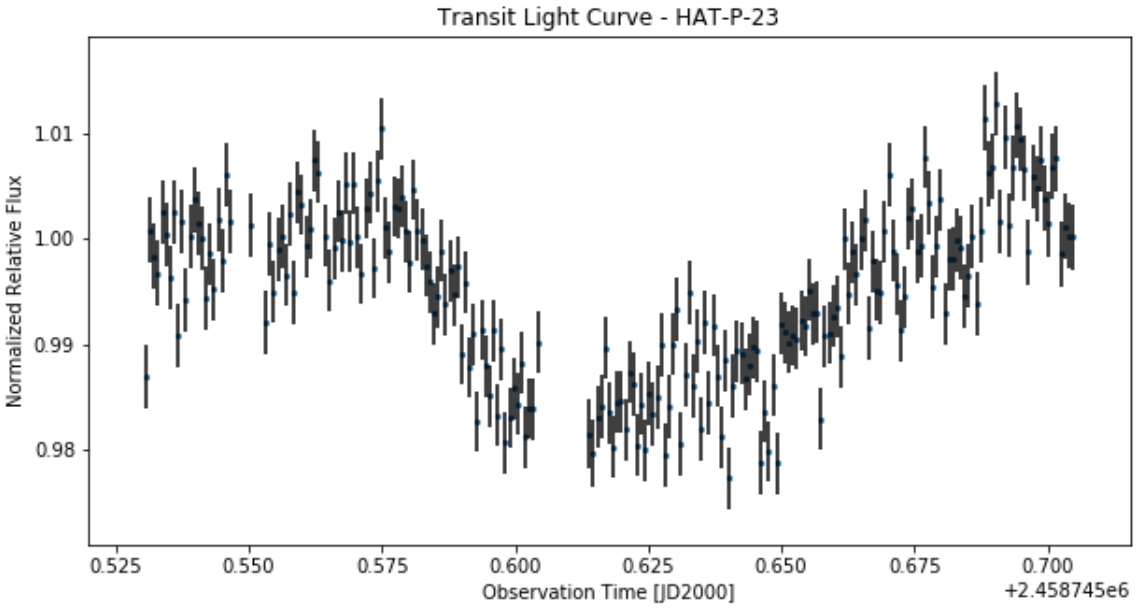

Figure 4. Normalized transit light curve of the HAT-P-23 system as observed from the 14-in telescope at Mt. Stony Brook Observatory. On the y-axis is the system flux after scaling with respect to reference stars, to correct for atmospheric effects, and normalizing by the system's baseline flux. Now, r represents the fraction of light from GSC 1632-01396 that is not obscured by the transit of HAT-P-23b. When out of transit, $r \approx 1.0$. During the transit, r is scattered about $1 - \epsilon$, where ϵ is the transit depth to be calculated.

The transit time prediction is confirmed by our data as it lies near the mid-point of our measured light curve. A more detailed prediction can be made using a Transit Ephemeris algorithm with orbital parameters determined by Bonomo et al. (2017), giving a mid-point time of 02:51 UT on September 19, 2019. This is only five minutes prior to our prediction and is still consistent with the observed light curve mid point.

The initial discovery of this transiting system was made using R-band photometric measurements, as we performed. A follow up survey by Ciceri et al. (2015) observed multiple transits of this system with a multi-band observation approach. Their observations used four optical filters spanning $400 - 900\ nm$, including an R-band filter. Our light curve measurement over one transit (Figure 4) gives a transit depth of $(1.333 \pm 0.022)\%$. This is smaller than the depth of $(1.364 \pm 0.238)\%$ reported by Bakos et al. (2011) but larger the $(1.325 \pm 0.001)\%$ depth reported by Ciceri et al. (2015). However, our measurement is still highly consistent within 0.1σ to both.

The initial discovery by Bakos et al. (2011) reports a planet radius of $R_p = (1.368 \pm 0.090) R_J$ and a star radius of $R_\star = (1.20 \pm 0.07) R_\odot$, corresponding to a planet-radius ratio of 0.1168 ± 0.0102. The multi-band follow up reports smaller radii of $R_p = (1.224 \pm 0.037) R_J$ and $R_\star = (1.09 \pm 0.03) R_\odot$. These measurements correspond to a radius ratio of 0.1151 ± 0.0047, which was shown to vary little over the range of filters used. Further, Sada & Ramón-Fox (2016) claim a ratio which is 4.5% smaller than that of Bakos et al. (2011), which suggests a value of 0.1115 ± 0.0097 for their measurement. In this report, we have determined the planet-radius ratio to be $(R_p/R_\star) = 0.1154 \pm 0.0009$. Our measurement is again highly consistent to within 0.36σ of each of these literature values.

The discovery report found a transit duration of $T = (2.17 \pm 0.02)$ h (Bakos et al. 2011). Our determination of $T = (2.20 \pm 0.09)$ h is highly consistent to 0.3σ. Since our measurement of the transit duration was less than the estimate derived from setting $b = 0$ in (2), we determined that the orbit of HAT-P-23b has a nonzero impact parameter. We did not independently measure the stellar radius, so we can not solve (2) to estimate the actual value of b. Bakos et al. (2011) measured a value for this parameter of $b = 0.32 \pm 0.07$. This value of the impact parameter is said to be nearly 'ideal'. Planets with $b = 0$ maximize the Rossiter-McLaughlin effect, causing large apparent variations in the host star's radial velocity that throw off measurements of it, while planets with large b have very short transit durations, making the transit difficult to observe. Therefore, transits with intermediate impact parameters are best for determining properties of the system. In the end, our measurement of the planet-star radius ratio of HAT-P-23 has strong agreement with measurements of the system made by Ciceri et al. (2015) and Bakos et al. (2011). Since we did not obtain an independent measurement of the radius of the host star GSC 1632-01396, we can not determine the physical radius of the planet nor make a determination on whether this planet is indeed a highly inflated Hot Jupiter. Previous literature reports HAT-P-23b having a mass $\approx 2\ M_J$. The observations by Ciceri et al. (2015) refined the stellar radius to a smaller value than reported in the initial discovery. Considering this given mass and our measurement of the planet-star radius ratio, the larger star radius reported in the initial discovery would suggest an inflated Hot Jupiter while the smaller star radius reported in the follow-up would suggest it is not inflated. We therefore can not make a definitive conclusion on this matter.

6. CONCLUSION

We have confirmed the transit of HAT-P-23b by observing one transit of the planet with duration of $(2.20 \pm 0.09)\ h$. The measured transit duration is less than that expected from an estimation assuming $b = 0$, so we determine that the planet has non-zero impact parameter, though an exact value can not be calculated without an independent measurement of the radius of GSC 1632-01396. Photometric measurements of this system with a red optical filter produced the transit light curve shown in Figure 4. We measured a transit depth of $(1.333 \pm 0.022)\%$ and a planet-star radius ratio of 0.1154 ± 0.0009. Our measurement of this ratio is smaller than reported in the system's initial discovery report (Bakos et al. 2011), but still finds strong agreement with it and follow up measurements of the system (Ciceri et al. 2015).

REFERENCES

Bakos, G. , Hartman, J., Torres, G., et al. 2011, The Astrophysical Journal, 742, 116, doi: 10.1088/0004-637x/742/2/116

Bonomo, A. S., Desidera, S., Benatti, S., et al. 2017, Astronomy Astrophysics, 602, A107, doi: 10.1051/0004-6361/201629882

Ciceri, S., Mancini, L., Southworth, J., et al. 2015, A&A, 577, A54, doi: 10.1051/0004-6361/201425449

Murphy, M., Isola, B., & Nill, T. 2019, Dark Current of the STL1001 Imaging CCD, Available at https://github.com/mm-murphy/CCD-Calibration

Sada, P. V., & Ramón-Fox, F. G. 2016, Publications of the Astronomical Society of the Pacific, 128, 024402, doi: 10.1088/1538-3873/128/960/024402

Tsantaki, M., Sousa, S. G., Santos, N. C., et al. 2014, A&A, 570, A80, doi: 10.1051/0004-6361/201424257

Wilson, P. A. 2016, The exoplanet transit method. https://www.paulanthonywilson.com/exoplanets/exoplanet-detection-techniques/the-exoplanet-transit-method/